Properties of Injected Plasmas in Indium Antimonide

BETSY ANCKER-JOHNSON,* ROGER W. COHEN, AND MAURICE GLICKSMAN
RCA *Laboratories, Princeton, New Jersey*

(Received August 2, 1961)

Plasmas composed of injected electron-hole pairs in p-type indium antimonide have been studied: The injection times have been measured. Pinching of the plasma has been observed. The current-voltage curves show a steep rise at voltages well below those required for breakdown, indicating a large increase in carrier density before breakdown. The Hall voltage measured as a function of current changed sign from that expected for hole transport to that expected for electron transport. Negative resistances have been observed in the plasma in the presence of transverse magnetic fields. Longitudinal magnetic fields decreased the plasma density, probably because of an increased radial diffusion of the plasma to the surface. Coherent oscillations have been observed on top of the pinch both with and without longitudinal fields. Their dependence on current and magnetic field is described.

INTRODUCTION

PREVIOUS work on electron-hole plasmas in InSb, a material chosen because of its relatively high carrier mobilities, has been performed by Glicksman, Steele, and Powlus of these laboratories.[1–4a] These workers have produced such plasmas in n-type InSb at 77°K by giving the electrons, the majority carriers in the crystal, sufficient energy to excite electron-hole pairs. The resulting current-voltage characteristics were examined as a function of time. Characteristically, a rise in resistance was observed a fraction of a microsecond after the impression of a high electric field. It is thought that the increase in resistance is caused by the plasma pinching down in a manner similar to gaseous plasmas. The existence of a critical current at which pinching begins was found consistent with the expression[5–7]

$$I_{cr}=20ck(T_e+T_h)/ev_d \text{ amp}, \quad (1)$$

where T_e and T_h are the mean kinetic temperatures of the electrons and holes, respectively, and v_d is the electron drift velocity in cm sec^{-1}. Also observed were coherent voltage oscillations on top of the pinch, and incoherent oscillations in the presence of an external longitudinal magnetic field.

Steele and Glicksman[3] also studied high-electric-field effects in p-type InSb. It was observed that the Hall coefficient changed sign from positive to negative as the current was increased. An analysis of the data yielded a value for the ratio of electron to hole mobilities. Their current-voltage curves showed a sharp upturn as was the case in the n-type work; however, the qualitative behavior of the curves was different. The p-type curves were not indicative of plasma pinching. Although their currents were greater than that necessary to produce self-pinch, they felt that the time required for the plasma to contract in their relatively impure sample (2.3×10^{16} cm^{-3}) was greater than their observation time, 0.25 μsec. Their suggestion that purer p-type samples should exhibit pinching as readily as the n-type InSb did led to the present work.

Carriers injected from current contacts into a p-type sample can make an appreciable contribution to the total carrier density. Since electron mobilities are so much greater than hole mobilities, the transit time for injected minority carriers in p-type material is shorter than the corresponding time in n type by more than an order of magnitude. The purer the p-type material, the more readily does injection occur. The present work was undertaken to study the properties of plasmas composed of carriers injected into a semiconductor.

EXPERIMENTAL ARRANGEMENT

The experimental arrangement employed for these measurements was the same as that of Glicksman and Powlus.[4] High current pulses were produced by discharging a coaxial line through the sample and a known series resistance under constant current conditions. A fast dual-beam oscilloscope with differential preamplifiers was used to observe the voltage drop across the specimen and across the known resistance so that the current and voltage were simultaneously observed as a function of time. The pulse duration was about 1 μsec and the repetition rate was less than 1 sec^{-1} to avoid heating the sample above its bath temperature, 77°K, at which all measurements were made.

The samples were single-crystal p-type InSb (unoriented) with initial hole concentrations between 1.1×10^{15} and 1.1×10^{18} cm^{-3}. They were cut into a bridge shape with asymmetrical current contacts as shown in Fig. 1. When the current was made to flow from the small to the large current contact, electrons injected from the lead at the large contact had a relatively long time and path length in which to recombine

* Present address: Boeing Scientific Research Laboratories, Seattle, Washington.

[1] M. Glicksman and M. C. Steele, Phys. Rev. **110**, 1204 (1958); M. C. Steele and M. Glicksman, J. Phys. Chem. Solids **8**, 242 (1959).
[2] M. Glicksman and M. C. Steele, Phys. Rev. Letters **2**, 461 (1959).
[3] M. C. Steele and M. Glicksman, Phys. Rev. **118**, 474 (1960).
[4] M. Glicksman and R. A. Powlus, Phys. Rev. **121**, 1659 (1961).
[4a] *Note added in proof*. See also A. G. Chynoweth and A. A. Murray, Phys. Rev. **123**, 515 (1961).
[5] W. Bennett, Phys. Rev. **45**, 890 (1930).
[6] L. Tonks, Phys. Rev. **56**, 360 (1939).
[7] P. C. Thonemann and W. T. Cowhig, Proc. Phys. Soc. (London) **B64**, 345 (1951).

TABLE I. Conductivities, Hall coefficients, concentrations, and mobilities of various samples.

No. (sample)	σ (ohm^{-1} cm^{-1})	$R_H\sigma$ (cm^2/v-sec)	p_h (cm^{-3})	p_l (cm^{-3})	μ_h (cm^2/v-sec)	μ_l (cm^2/v-sec)
1 (101-D)	107	640	1.1×10^{18}	...	640	...
2 (101-5)	89	935	6.0×10^{17}	...	935	...
3 (80-V)	11.5	3630	2.0×10^{16}	4.2×10^{13}	3490	42 000
4 (190-C-1-4)	2.67	8250	2.1×10^{15}	1.0×10^{13}	8000	79 000
5 (190-D-1-3)	1.19	6880	1.1×10^{15}	2.3×10^{12}	6670	97 000

before arrival at the region of the crystal under observation. This resulted in a relatively low level of injection. When the current direction was reversed the density of injected minority carriers was made appreciably higher. Thus, by choosing an appropriate location for the electron injecting contact, the level of injection was readily varied.

EXPERIMENTAL RESULTS

A. Properties at Low Levels of Current Density

The conductivities of the various samples studied are shown in Table I. The Hall coefficients, R_H, were measured as a function of magnetic field. Hole concentrations deduced from these measurements are tabulated in column 4 and the Hall mobility is listed in column 3. Samples with a greater concentration of holes than about 10^{17} cm^{-3} had essentially constant Hall coefficients over the available range of field strengths. The purer samples exhibited a strong magnetic field dependence as demonstrated in Fig. 2 which shows, as an example, the Hall curve for crystal No. 4. (All the data quoted refer to crystal 4 unless otherwise stated). At large magnetic fields the magnitude of R_H is slightly greater for higher injection levels even at the small current used, 10 ma. Since the free electron density was much too small to produce the observed variation in R_H with H, light holes are assumed to be responsible for this effect. An analysis, to be described in another paper,[8] of the R_H vs H curve has yielded the concentration p_l and mobility μ_l of light holes as well as the corresponding quantities for heavy holes, p_h and μ_h (see Table I).

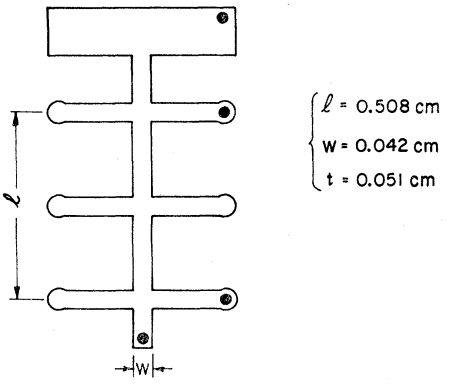

FIG. 1. The sample shape showing asymmetrical current contacts and typical dimensions (exact for crystal 4).

[8] B. Ancker-Johnson and R. W. Cohen, (to be published).

B. Properties of Injected Plasmas

1. *Evidence for Injection*

Figure 3(a) illustrates the crystal behavior at high levels of current density. In this photograph the current pulse is the lower waveform while the simultaneous voltage response is shown above. The voltage rose initially to a maximum value and then decreased sharply after a time τ_i. After a further time τ_p, it rose to what was apparently a steady-state value about which it oscillated in a coherent manner, as shown in Fig. 3(b). This waveform is very similar to that seen by Glicksman and Powlus[4] in n-type InSb. Their work indicated that the resistance decrease after τ_i was caused by breakdown and the resistance increase after τ_p was caused by pinching. Their observations were made at fields large enough to cause impact ionization; in the present case, however, the fields were well below those needed to produce breakdown, as will be discussed in Sec. 1(c). The following experimental evidence indicates that a plasma has been produced in a crystal by injection of electrons from a current contact and the subsequent accumulation of compensating holes:

(a) The finite time τ_i for which the sample showed a marked enhancement in conductance agrees well with that predicted by a theory assuming injection of electron-hole pairs.

(b) The behavior of the critical current for pinching, I_{cr}, with varying injection level is consistent with theory.

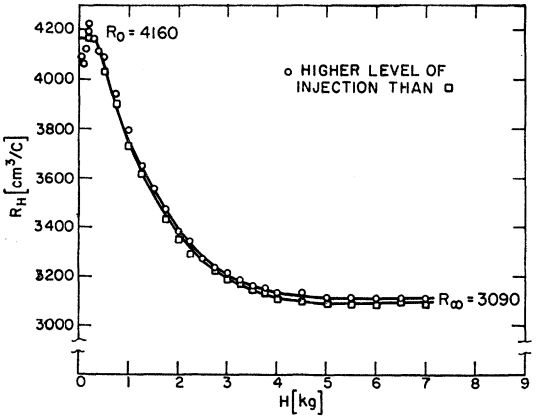

FIG. 2. The magnetic field dependence of the Hall coefficient at a low current level (10 ma) for crystal 4 whose hole concentration is 2.1×10^{15} cm^{-3}.

(c) The current-voltage curves display a marked rise in conductance at fields well below those needed to produce impact ionization.

(d) Measurements of the Hall coefficient R_H as a function of current through the sample show that R_H changed sign from positive for low currents to negative for high currents.

(*a*) *Injection time.* When electrons are injected from a contact into p-type material, they are driven by the applied field E to drift into the sample at their natural drift velocity $\mu_e E$. However, if only electrons were injected with density n comparable to the equilibrium density of holes p_0, large fields would be produced inside the crystal because of space charge. Therefore, a roughly equal number of compensating holes must be associated with the injected electrons in order to conserve space-charge neutrality. These holes may emerge from the same contact as the electrons or from the region of the crystal surrounding the contact, in which case they are ultimately replaced from the opposite contact. There results a neutral electron-hole cloud or plasma moving down the crystal at some velocity V which one expects to be a function of the injected density n. V should be less than the free-electron drift velocity because of the tendency of the holes in the plasma to travel in a direction opposite to that of the plasma.

Following Herring[9] it is assumed that:

(1) $$p=n+p_0, \tag{2}$$

which ensures that the net space charge is zero and hence the number of injected electrons n is equal to the number of injected holes, $p-p_0$.

(2) The lifetime of the minority carriers is much greater than any other time concerned in this process. That this assumption is justified is evident from the fact that plasma effects have been observed.

(3) Diffusion currents can be neglected in comparison with the currents driven by the impressed electric field.

(4) The equilibrium concentration of electrons n_0 is much less than p_0.

Under these conditions Herring[9] found that an injected plasma will propagate according to the following nonlinear partial differential equation:

$$\partial n/\partial t=-V(n)\partial n/\partial x, \tag{3}$$

where

$$V(n)=\frac{\mu_e E}{[1+(b+1)n/p_0]^2}, \tag{4}$$

$$b=\mu_e/\mu_h, \tag{5}$$

and x is the linear dimension along which the plasma propagates.

The Ohmic current is

$$I_\Omega=ep_0\mu_h EA, \tag{6}$$

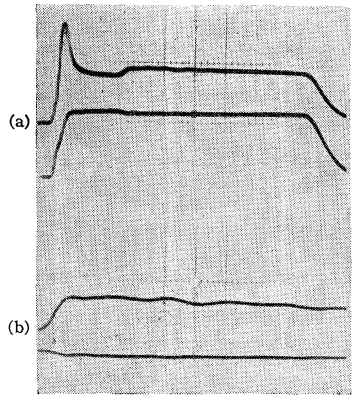

FIG. 3. (a) Voltage (above) and simultaneous current pulses proportional to the voltage drop across the crystal and current through it, respectively. A repetition of three pulses was used to make the oscillogram. t: 0.1 μsec/cm; V: 50 v/cm; $I=5.0$ amp. (b) Same as in (a) except magnified 5× in amplitude and 2½× in time scale. t: 0.04 μsec/cm; $\nu\approx14$ Mc/sec. Five pulses were used.

where A is the sample cross-sectional area. The total current is

$$I_T=ep_0\mu_h EA[1+(b+1)n/p_0]. \tag{7}$$

Hence, $V(n)$ can be rewritten in the form

$$V(n)=\mu_e E(I_\Omega/I_T)^2. \tag{8}$$

If the plasma pulse travels a distance L while passing through the region where the field is being measured, the time for the pulse to traverse this distance is simply

$$\tau_i=L/V(n)=(L/\mu_e E)(I_T/I_\Omega)^2. \tag{9}$$

The injection time τ_i is the time required for the voltage to drop from its maximum to a steady state as illustrated in Fig. 3(a). If a value for the electron mobility of 2.0×10^5 cm^2/v-sec is assumed, a reasonable value[10] when $p_0=2.0\times10^{15}$ cm^{-3}, τ_i can be calculated. L was approximately equal to 0.5 cm. Table II shows the calculated values of the injection times compared with the experimental values for the experimental arrangement with which the longest injection times occurred. This corresponded to minimal injection of plasma.

There is good agreement between the measured τ_i and those calculated from Herring's theory which supports

TABLE II. Injection times for the lowest injection level.

E (v/cm)	$(I_T/I_\Omega)^2$	$\tau_{i\,\mathrm{calc}}$ (μsec)	$\tau_{i\,\mathrm{exp}}$ (μsec)
300	7.55	0.063	0.06
280	7.48	0.067	0.06
275	7.52	0.068	0.07
255	7.51	0.074	0.07
234	7.57	0.081	0.08
198	7.90	0.098	0.10
176	7.30	0.104	0.11
167	6.55	0.100	0.11

[9] C. Herring, Bell System Tech. J. **28**, 401 (1949); see also W. Shockley, *Electrons and Holes in Semiconductors* (D. Van Nostrand Company, Inc., New York, 1950), 328f.

[10] E. H. Putley, Proc. Phys. Soc. (London) **73**, 280 (1959).

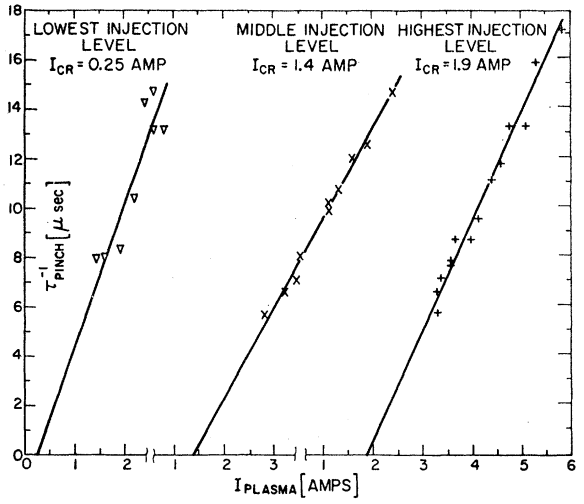

FIG. 4. Plot of inverse pinch time versus plasma current for three different injection levels.

the view that an injected plasma has been produced in the experiments. Since the reduction factor for the velocity in these measurements was about 7.5, use of the free-electron drift velocity rather than the plasma velocity would have yielded τ_i's a factor of 7.5 smaller than those observed.

(*b*) *Pinch time.* Measurements of pinch time τ_p as a function of the plasma current

$$I_p = I_T - I_\Omega \tag{10}$$

have been carried out for three different levels of injection.[11] As in the case of the studies on *n*-type InSb, it is expected that τ_p should depend on the current approximately through the relation[12]

$$\tau_p = A(I_p - I_{cr})^{-1}, \tag{11}$$

where I_{cr} is given by Eq. (1). However, I_{cr} was not in general a constant during any one experimental run as it was in the *n*-type experiments, since the electric field increased as the current increased (compare Fig. 5). Thus, the electron drift velocity v_d which appears in I_{cr} was a function of I_p. This was also the case for the parameter A, which would depend on the electron drift velocity and the radial mobility of the plasma (μ_r) in pinching, i.e.,

$$A \approx 10^9 a^2/2v_d\mu_r. \tag{12}$$

The observed values of τ_p^{-1} are plotted as a function of I_p in Fig. 4. The electric fields applied in these measurements were in the range 165–445 v/cm; for these values, the drift velocity is probably increasing only slowly with the electric field, since saturation was observed for fields in this range in *n*-type InSb.[1] The curves are best-fit straight lines, for each set of points, and the resulting values of A and I_{cr} are listed in Table III. It should be noted that the v_d which appears in Eq. (1) should be practically independent of injection level, since it corresponds to the current-carrying velocity of the plasma when it occupies the entire length of the semiconductor. However, μ_r will be equal to $V(n)/E_r$, and will be a rather complicated function of injected density and time during the pinching process. The last column of Table III contains the values of v_d which satisfy Eq. (1), with $k(T_e+T_h)$ set equal to $2kT$ and $T=77°$K. Actually, T may be larger than 77°K because of the expected heating of the plasma electrons at the fields used.

TABLE III. Analysis of pinch-time data.

Injection level	A (coul)	I_{cr} (amp)	Calculated drift velocity (cm/sec)
Lowest	1.7×10^{-7}	0.25	1.1×10^{8}
Intermediate	2.7×10^{-7}	1.4	1.9×10^{7}
Highest	2.2×10^{-7}	1.9	1.4×10^{7}

The values calculated for v_d at the intermediate and highest injection levels are reasonable, but the value which comes from the lowest injection observations appears inordinately large. These latter data contained the largest scatter, and the value for I_{cr} is the least accurate of those listed in the Table III. The "average" value of μ_r, as calculated using Eq. (12) and the values of A listed in the table, is about 5×10^4 cm²/v-sec.

(*c*) *Current-voltage characteristics.* Figure 5 shows the current-voltage characteristics for three levels of injection. At low fields all three curves follow an Ohmic

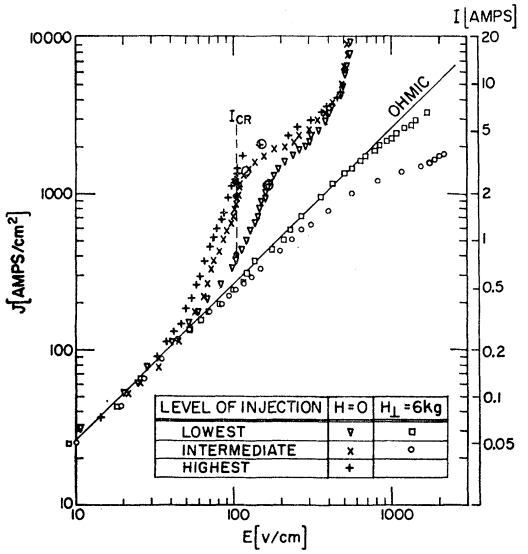

FIG. 5. Conductivity characteristics for the three levels of injection used to obtain the data in Fig. 4. Also shown are the current-voltage curves in a transverse magnetic field of 6000 gauss for the two lowest injection levels. The filled circles correspond to the critical currents for pinching at each injection level. The large open circles indicate the lowest J-E magnitudes at which pinching was observed.

[11] B. Ancker-Johnson and R. W. Cohen, Bull. Am. Phys. Soc. **6**, 311 (1961).
[12] M. Glicksman (unpublished); see also reference 4.

TABLE IV. Density of injected carriers when pinch first observed.

Injection level	I_{plasma} (amp)	n/p_0	$n(cm^{-3})$
Lowest	1.4	0.060	1.3×10^{14}
Intermediate	2.8	0.106	2.2×10^{14}
Highest	3.3	0.146	3.1×10^{14}

law that corresponds to the zero-field conductance. Departures from the Ohmic line begin at approximately 50 v/cm. Thereafter the conductivity exhibits a sharp rise. This rise is attributed to the injection of an electron-hole plasma from the current contacts as discussed in the preceding sections. The various levels of injection were determined by the amount of current flowing through the sample at a given field, the higher injection level permitting the flow of more current.

The departure of the curves from the Ohmic line continues to increase until a gradual flattening occurs in the region between 105 and 180 v/cm depending on the level of injection. At these voltages, the rise in resistance indicative of pinching was first observed. The flattening of the curves occurred because the cross-sectional area carrying the current was reduced from the geometrical cross section to the pinch cross section. Since the former was the value used to compute J, the values of J at fields above those where pinching was observed are in error by an amount equal to the ratio of the geometrical area to the pinched area.

From Fig. 5 it is seen that the curves converge at the breakdown voltage, approximately 500 v/cm, where the current rose very steeply. The injected carriers have become energetic enough to excite additional electron-hole pairs by impact ionization.

The density of injected carriers, n, may be estimated at any field below that where flattening of the curves begins by reading the total current I_T and the Ohmic I_Ω directly from the graph and substituting these values into the equation obtained by combining Eqs. (6) and (7):

$$I_T/I_\Omega=1+(b+1)n/p_0. \tag{14}$$

Table IV lists the values of n at the points where pinching was first observed, for the three different levels of injection. It was assumed that the mobility ratio b is 25, which is correct for the crystal under consideration if[10] $\mu_e=2.0\times10^5$ cm²/v-sec, since $\mu_h=8000$ cm²/v-sec (cf. Table I). The values of the plasma density at the onset of self-pinching are comparable to those seen in a strong gaseous discharge.

The conductivity curves for crystal 3, $p_0=2.0\times10^{16}$ cm^{-3}, show only a very slight deviation from Ohmic behavior beginning at 240 v/cm. At ~300 v/cm pinch was first observed. Insufficient pinch time measurements could be made to allow determination of I_{cr}. No hump attributable to injection could be observed in the still less pure samples, nor was it possible to see any signs of pinching in the time observations of the voltage pulse. It was apparently not possible to produce an injected plasma of significant density in samples with p_0 much larger than 2×10^{16} cm^{-3}.

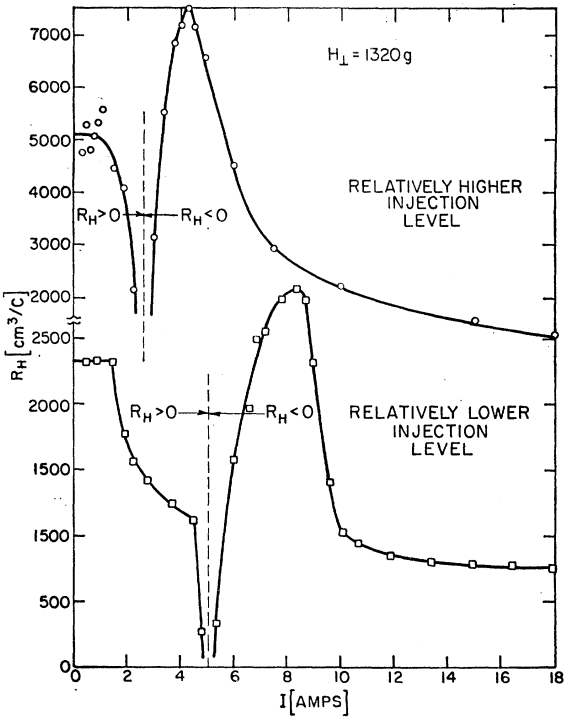

FIG. 6. A plot of Hall coefficient versus total current for two levels of injection corresponding to the intermediate and lower injection levels of Figs. 4 and 5.

(*d*) *Dependence of the Hall coefficient on current.* Figure 6 illustrates, at $H=1320$ gauss, the dependence of the Hall coefficient R_H on the total current I_T for two levels of injection. R_H is initially positive but soon drops to zero, reaches a maximum negative value and falls off rapidly, then slowly at high currents. The observed change of sign of the Hall coefficient is further evidence of injection. The current for which $R_H=0$ is larger for the lower injection than for the higher injection cases, independent of H, because a larger current is necessary for injection of the same number of electron-hole pairs.

The condition for $R_H=0$ may be obtained by substituting Eq. (2) into the Hall coefficient expression[13]

$$R_H=\frac{p-nb^2+b^2\mu_h^2H^2(p-n)}{e[(bn+p)^2+b^2\mu_h^2H^2(p-n)^2]}, \tag{15}$$

where b is the mobility ratio, Eq. (5), at $H=0$. Solving Eq. (15) for $R_H=0$ yields

$$n/p_0=(1+\mu_e^2H^2)/(b^2-1). \tag{16}$$

In this particular example, $H=1320$ gauss, and again assuming that μ_e is 2.0×10^5 cm²/v-sec, the result is $n/p_0=0.013$. Thus, only a relatively small number of injected electrons is required to change the sign of the

[13] R. A. Smith, *Semiconductors* (Cambridge University Press, New York, 1959), 106.

TABLE V. Effect of a transverse magnetic field on injected density.

		Lowest Injection Level			Intermediate Injection Level		
H (gauss)	n/p_0 at $R_H=0$	I_T for $R_H=0$ (amp)	n/p_0 for $H=0$	% Reduction in n	I_T for $R_H=0$ (amp)	n/p_0 for $H=0$	% Reduction in n
200	0.0018	1.50	0.038	95	0.45	0.011	84
660	0.0044	3.85	0.093	~95	1.85	0.089	95
1320	0.013	5.05	0.114	~89	2.55	0.118	~89
2000	0.027	5.30	0.118	~77	3.20	0.146	~82
6000	...	[a]	...	100	[a]	...	100

[a] The Hall coefficient did not change sign for $I \leq 15$ amp.

Hall coefficient. The falling off of the negative R_H at high currents occurs when the injection level is so high that $n \gg p_0$ and

$$R_H \xrightarrow[n \gg p_0]{} -\frac{1}{ne}\frac{b-1}{b+1} \approx -\frac{1}{ne}. \tag{17}$$

The bend in the curve for low injection level in the region between 1.5 and 4.5 amp, which is present also in plots of R_H vs I for other values of H, is as yet unexplained.

The effect of a transverse magnetic field on injected density has been found by comparing the values of n/p_0 obtained through the use of Eq. (16) to those calculated by Eq. (14) in which the values of I_T for which $R_H=0$ were employed. The results are given in Table V. The n/p_0 values for $H=0$ are only approximate at the higher I_T because of uncertainty in the ratio I_T/I_Ω. The Table V shows that the density of the plasma is greatly reduced by the application of a transverse magnetic field. In fact, a magnetic field of only 200 gauss succeeded in preventing about 84% of the injected carriers in the intermediate injection level case from reaching the region where the Hall voltage was measured and 95% in the lowest injection case. This effect is due to the carriers being swept to the surface where they can readily recombine. The Hall angle at 200 gauss was approximately 20°. Since the crystal was 0.042 cm wide, the carriers traveled only about 0.1 cm down the crystal before they were destroyed. Magnetic field effects are discussed further in the next section.

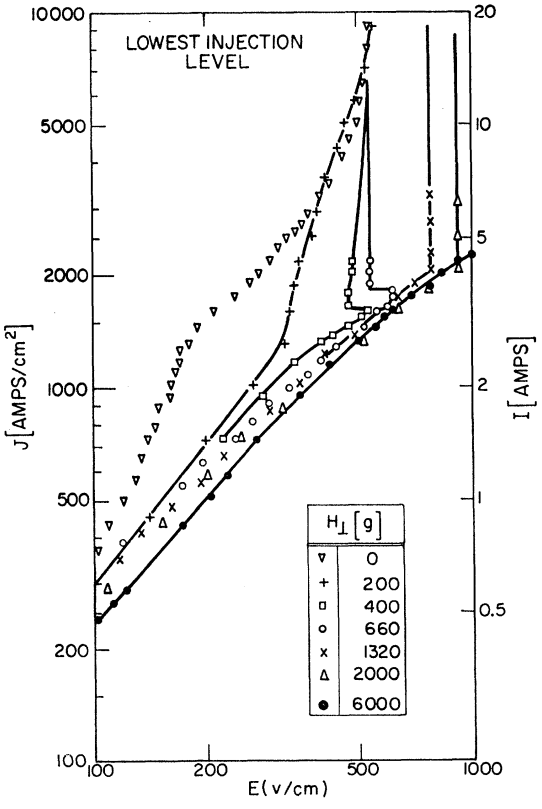

FIG. 7. Conductivity curves in transverse magnetic fields at an injection level corresponding to the lowest injection level of Fig. 5.

2. *Properties of Injected Plasmas in the Presence of Magnetic Fields*

(*a*) *Transverse fields.* The conductivity characteristics of the injected plasma were drastically modified by the presence of both transverse and longitudinal magnetic fields. Either field, if large enough, inhibited or destroyed the pinch and flattened the humps in the *J-E* curves that were caused by injection.

In a large transverse field the conductivity for a sufficiently low level of injection remained Ohmic at electric field strengths considerably larger than the breakdown electric field in zero magnetic field, E_0, as shown in Fig. 5. Whereas for $H=0$ and a relatively low level of injected carriers, an increase in conductivity was observable at a few tens of volts/cm, in a transverse field of 6 kgauss the conductivity was Ohmic up to field strengths at least 300 v/cm beyond E_0. This transverse field thus was sufficient to sweep the injected carriers to the surface where they recombined. At still higher voltages the conductivity began to *decrease*. Also, as the level of injection was raised (circles in Fig. 5), a reduction in conductivity was observed to begin at lower voltages than was the case for lesser injection. These smaller values of conductivity may be attributed to a reduced mobility expected at high electric fields and large carrier concentrations. A voltage of $4E_0$ was not sufficient under these conditions to initiate breakdown.

At intermediate transverse magnetic fields negative resistance regions were observed in the J-E characteristics, Figs. 7 and 8. In a transverse field of 200 gauss and for the lowest level of injection (Fig. 7) the conductivity departed from Ohmic behavior at low voltages, but not so markedly as in the zero-field case. Hence a fraction of the injected carriers was lost by recombination at the surface, in agreement with the Hall data. Eventually, the injected electrons produced an avalanche of electron-hole pairs by impact ionization at E_0. At 400 gauss the magnetic field was more effective in sweeping out injected carriers so that an electric field in the vicinity of E_0 was reached without significant departure from Ohmic behavior. A slight further increase in the current, however, caused a sudden reduction in voltage to E_0. In the presence of 660 gauss the voltage reached a magnitude about 70 v/cm beyond E_0 before it suddenly dropped to E_0 and breakdown occurred. This negative resistance occurred because the magnetic field swept the injected carriers to the surface sink so that a voltage could be sustained in the crystal greater than E_0. As the voltage was increased further some injected electrons survived to acquire the high velocities dictated by the impressed voltage. They immediately initiated breakdown at E_0. A further rise in magnetic strength

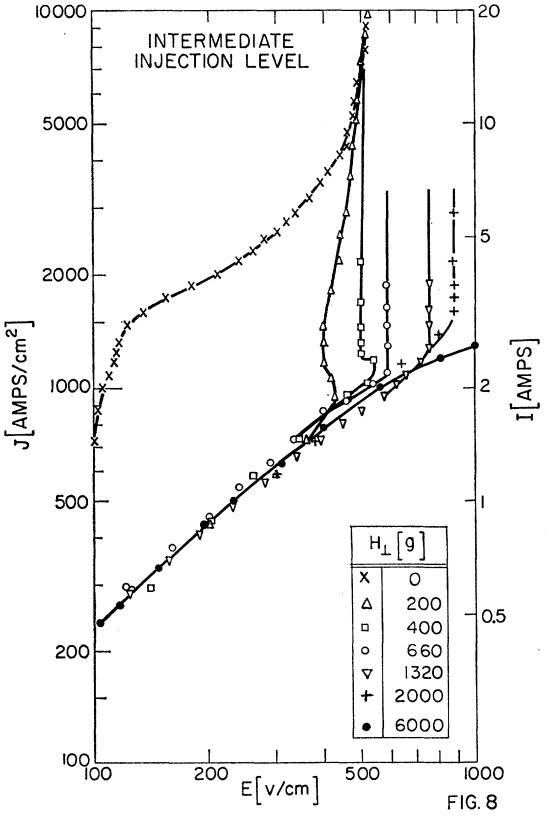

FIG. 8. Conductivity curves in transverse magnetic fields at an injection level corresponding to the intermediate injection level of Fig. 5.

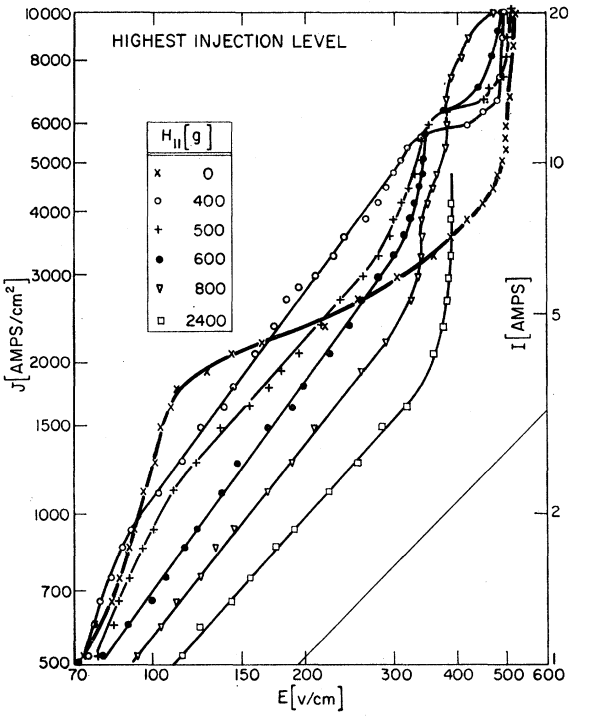

FIG. 9. Conductivity curves in longitudinal magnetic fields at an injection level corresponding to the highest injection level of Fig. 5. The full line represents Ohmic conductivity.

was still more effective in preventing injected carriers from contributing to the conductivity (compare Table V) and breakdown resulted at higher voltages than E_0, depending on the magnetic field.

The magnitudes of the threshold voltages current densities and magnetic fields at which negative resistance occurred were *lower* as the density of injection was raised (compare Figs. 7 and 8). Why this shift takes place is not yet understood. The electron mobility was certainly reduced in the higher injection case as compared to the lower. For electrons to acquire the same velocity in the two situations, a *higher* voltage would be expected in the higher injection case. Also, since the Hall angle is approximately equal to μH, a *higher* magnetic field should be required to produce the same effectiveness in sweeping out carriers. The observations were surely of long enough duration (1 μsec) to allow the carriers to traverse the distance to the surface, on the average $\sim$0.02 cm, even though their velocity was reduced by $(I_\Omega/I_T)^2$. Hence, the shift to lower thresholds with higher carrier concentrations is puzzling.

(*b*) *Longitudinal fields.* Pinching was destroyed by the impression of a sufficiently large longitudinal magnetic field. It ceased being detectable by time observations of the voltage pulse at a field of approximately 350 gauss (cf. Fig. 11). The conductivity characteristics of the injected plasma in the presence of longitudinal fields up to 2.4 kgauss (maximum available) are shown in Fig. 9. These curves coalesce to the

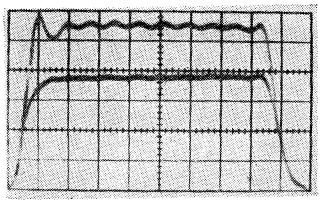

$p_0 = 2.0 \times 10^{16}$ cm^{-3}

FIG. 10. Voltage (above) and current pulse obtained using crystal 3 at 10.6 amp. $V \sim 10$ v/cm; t: 0.04 μsec/cm; $\nu \approx 32$ Mc/sec. A repetition of three pulses was used to produce the photograph.

Ohmic J-E curve at a few tens of volts/cm. The hump caused by injection in the zero-field case is increasingly flattened as the magnitude of H is raised and Ohmic behavior is approached up to high electric fields. Breakdown occurs at the zero-field breakdown electric field independently of $H_{\parallel}$. In between breakdown and the flat part of the J-E curve, humps occur at larger J and E values as $H_{\parallel}$ is increased, but become less pronounced. These humps suggest that pinching was occurring although its time dependence could not be observed because the pinch time was too short. The cause of the steep rise in current before the humps occur at the higher $H_{\parallel}$ values is not understood.

Kadomtsev and Nedospasov[14] have proposed a type of helical hydromagnetic instability to explain the anomalous diffusion in gaseous plasmas. An incipient helical distortion of the plasma is shown to grow, producing oscillations and an increased velocity of the electrons transversely to the applied $H_{\parallel}$. Glicksman[15] has suggested that these instabilities are the source of oscillations observed in semiconductors containing electron-hole plasmas and has modified the Kadomtsev-Nedospasov theory for application to such plasmas.

The magnitude of the transverse drift or diffusion velocity $V_{\perp}$ accompanying such a helical distortion will determine the extent of loss of injected plasma by recombination at the crystal surfaces, and hence, the extent to which the J-E characteristics approach Ohmic behavior. For the contribution of the injected carriers to the conductivity to be diminished $V_{\perp} \gtrsim 0.04 V_{\parallel}$ as dictated by the geometry (cf. Fig. 1). At 100 v/cm, before pinching occurred in the absence of a field, $V_{\parallel} = 9.4 \times 10^5$ cm/sec for the highest injection level of Fig. 5, assuming again that $\mu_e = 2.0 \times 10^5$ cm^2/v-sec.

TABLE VI. Effect of longitudinal magnetic fields on the intermediate injection level.

$H_{\parallel}$ (gauss)	J_T (amp/cm^2)	n/p_0	% Reduction in n	$V_{\perp}$ (cm/sec)
0	1230	0.139	0	0
400	1080	0.117	16	0.6×10^4
500	920	0.094	32	1.2
600	670	0.058	58	2.2
800	570	0.044	68	2.5
2400	445	0.026	81	3.1

Thus, for an appreciable loss of injected carriers $V_{\perp}$ would have to be at least 3.8×10^4 cm/sec. Table VI shows the percentage reduction of injected carriers for the various longitudinal magnetic fields employed and also the calculated minimum transverse velocity that would account for such a reduction. It is seen that $V_{\perp}$ rises rapidly with applied H and then saturates. If the percentage loss of carriers is the same at three times this electric field strength, i.e. $E \approx 300$ v/cm, $V_{\perp}$ reaches a minimum value of 5.5×10^5 cm/sec for the 2.4-kgauss case just before the rapid rise in current occurs.

(*c*) *Oscillations.* As shown in Fig. 3(b), coherent oscillations were observed on top of the pinch. Another example is shown in Fig. 10 for an order of magnitude higher initial density of holes (crystal 3). This oscillogram also differs from Fig. 3 in that it was taken at a higher current, and hence the pinch time was much shorter.

It was observed (for any one level of initial hole density) that the oscillation frequency increased as the current level was raised. These oscillations may be attributed[16] to standing hydromagnetic waves.[17] Calculations[18] show that the frequency should be proportional approximately to the square root of the current or carrier density, in general agreement with these results.

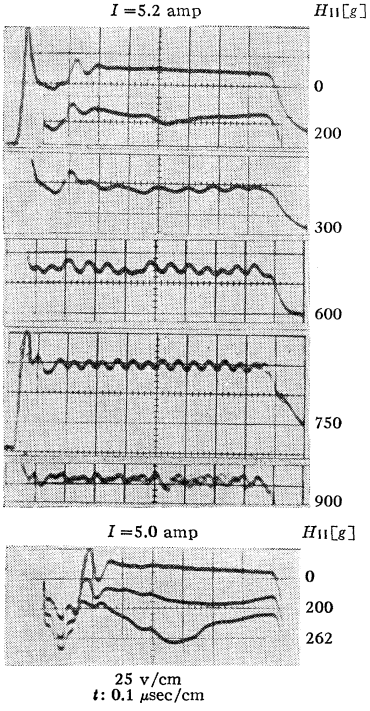

FIG. 11. Voltage pulses at a constant current and varying longitudinal magnetic field ($E = 4 \times$v). Each photograph corresponds to three pulses.

[14] B. B. Kadomtsev and A. V. Nedospasov, J. Nuclear Energy **1**, 230 (1960).

[15] M. Glicksman, Bull. Am. Phys. Soc. **6**, 116 (1961); this issue [Phys. Rev. **124**, 1566 (1961)].

[16] The authors wish to thank R. Gajewski for this suggestion.

[17] H. Alfvén, Arkiv Mat. Astron. Fysik **29B**, No. 2 (1942); see also L. Spitzer, Jr., *Physics of Fully Ionized Gases* (Interscience Publishers, New York, 1956), No. 3, p. 55ff.

[18] M. Glicksman, Bull. Am. Phys. Soc. **6**, 115 (1961).

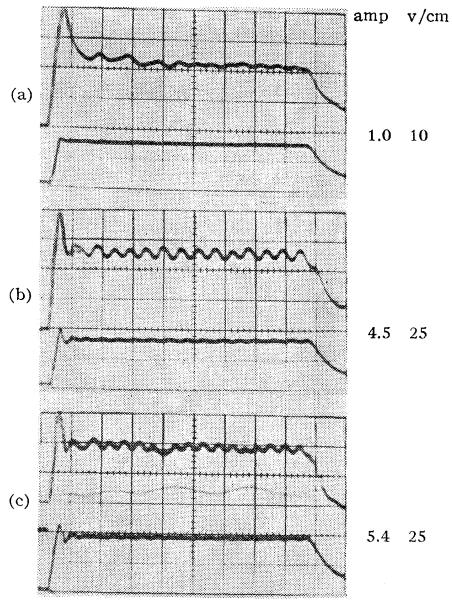

FIG. 12. Voltage pulses ($E=4\times$v) at a constant longitudinal magnetic field and varying current whose value is obtained from the lower pulse in each oscillogram. Each photograph corresponds to three pulses. $H_{\parallel}=700$ gauss; t: 0.1 μsec/cm.

The application of a moderate $H_{\parallel}$ enhances the amplitude of the oscillations as expected if a helical hydromagnetic wave grows.[14] Figure 11 shows the voltage response at a fixed current as $H_{\parallel}$ was increased. A long-wavelength oscillation was superimposed on the zero-field oscillations of about 14 Mc/sec as $H_{\parallel}$ approached 200 gauss. Although several frequencies were observed in fields up to about 700 gauss, they were coherent from pulse to pulse. Pinch was completely masked beyond about 350 gauss, if it occurred at all. At 750 gauss for the particular current chosen, only one frequency was observed, $\nu\approx 20$ Mc/sec. Further increase in $H_{\parallel}$ produced oscillations that were no longer coherent.

Figure 12 shows the oscillation behavior as a function of current in a fixed magnetic field. Several superimposed coherent frequencies are again observed in general, but also there is a particular current value for which only a single frequency occurs. The frequency increases with current.

SUMMARY

A plasma composed of injected electrons and holes of controllable density has been produced at least 350 v/cm below the breakdown voltage. The measured injection times agree well with those predicted by Herring's theory. Self-pinching of the plasma has been observed by time observations of a voltage pulse across the sample. The measured pinch times are consistent with Bennett's theory. The presence of an injected plasma was shown to be associated with a J-E curve which characteristically exhibits a steep rise in current at voltages well below those required for impact ionization. The densities of the injected plasmas at the onset of self-pinching were calculated. Hall measurements as a function of current showed that only a small fraction of injected electrons, less than 0.1%, is required to produce a reversal of Hall voltage.

Negative resistances were observed in the presence of moderate transverse magnetic fields, dependent on their magnitude and that of the applied voltage, as well as the injection level. The effectiveness of the magnetic field in sweeping injected carriers to the surface accounts for the existence of a negative resistance, but the observed dependence on injection level is not yet understood. Longitudinal magnetic fields were also effective in reducing the injected density, in general agreement with the proposal that hydromagnetic instabilities are induced, with a resulting increased transverse diffusion.

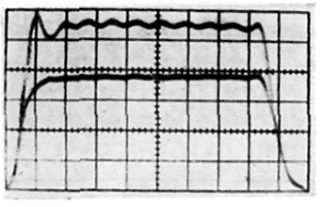

$p_0 = 2.0 \times 10^{16}$ cm^{-3}

FIG. 10. Voltage (above) and current pulse obtained using crystal 3 at 10.6 amp. $V \sim 10$ v/cm; t: 0.04 μsec/cm; $\nu \approx 32$ Mc/sec. A repetition of three pulses was used to produce the photograph.

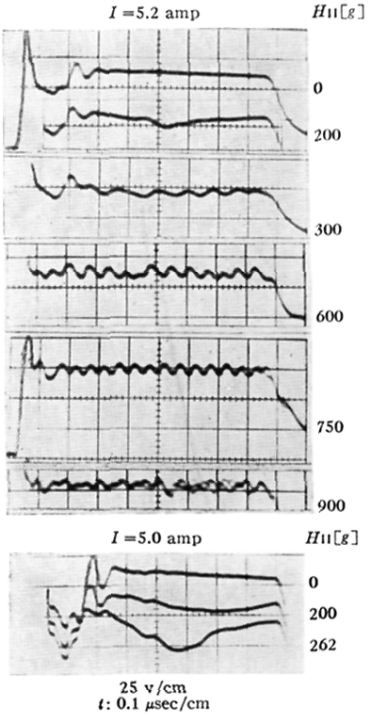

FIG. 11. Voltage pulses at a constant current and varying longitudinal magnetic field ($E=4\times$v). Each photograph corresponds to three pulses.

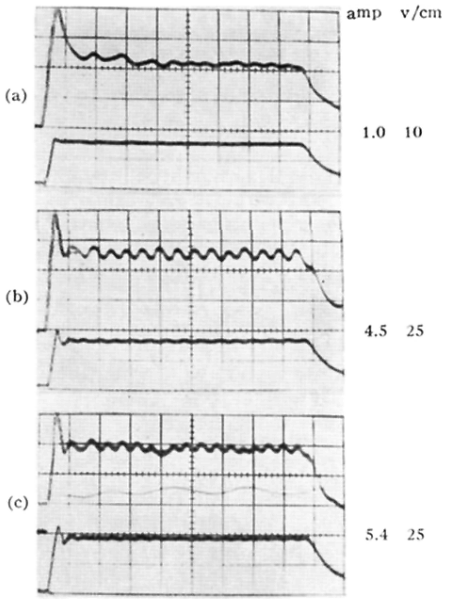

FIG. 12. Voltage pulses ($E=4\times$v) at a constant longitudinal magnetic field and varying current whose value is obtained from the lower pulse in each oscillogram. Each photograph corresponds to three pulses. $H_{11}=700$ gauss; t: 0.1 μsec/cm.

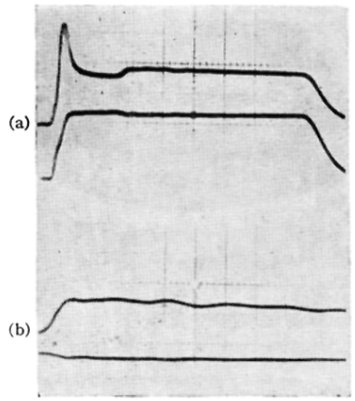

$p_0 = 2.0 \times 10^{15}$ cm^{-3}

FIG. 3. (a) Voltage (above) and simultaneous current pulses proportional to the voltage drop across the crystal and current through it, respectively. A repetition of three pulses was used to make the oscillogram. t: 0.1 μsec/cm; V: 50 v/cm; $I = 5.0$ amp. (b) Same as in (a) except magnified 5× in amplitude and 2½× in time scale. t: 0.04 μsec/cm; $\nu \approx 14$ Mc/sec. Five pulses were used.